Int. J. Electrochem. Sci., 15 **(2020)** 10463 – 10475, doi: 10.20964/2020.10.29

International Journal of
ELECTROCHEMICAL
SCIENCE
www.electrochemsci.org

Polythiopene/copper bismuthate nanosheet nanocomposites modified glassy carbon electrode for electrochemical detection of benzoic acid

X. Y. Guo[1], Y. J. Mao[1], C. H. Yu[1], F. L. Qiu[1], L. Z. Pei[1,], X. Z. Ling[2,*], Y. Zhang[3], M. C. Wang[4], and C. G. Fan[1]*

[1] Key Laboratory of Metallurgical Emission Reduction & Resources Recycling, Ministry of Education, School of Materials Science and Engineering, Anhui University of Technology, Ma'anshan, Anhui 243002, P. R. China
[2] School of Civil Engineering, Harbin Institute of Technology, Heilongjiang, Harbin 150090, P. R. China
[3] The Key Laboratory for Power Metallurgy Technology and Advanced Materials of Xiamen, Xiamen University of Technology, Xiamen, Fujian 361024, P. R. China
[4] College of Chemistry and Chemical Engineering, Hainan Normal Technology, Haikou, Hainan 571158, P. R. China
[*]E-mail: lzpei1977@163.com (L. Z. Pei), ling_xianzhang@163.com (X. Z. Ling).

Received: 8 June 2020 / *Accepted:* 19 July 2020 / *Published:* 31 August 2020

An *in-situ* polymerization method was developed to fabricate polythiophene/copper bismuthate nanosheet nanocomposites. The obtained nanocomposites were analyzed by X-ray diffraction (XRD) and transmission electron microscopy. The nanocomposites with the size of several hundreds of nanometers are composed of tetragonal $CuBi_2O_4$ phase. Amorphous polythiophene nanoparticles attach to the surface of the polycrystalline copper bismuthate nanosheets. A glassy carbon electrode (GCE) modified with the polythiophene/copper bismuthate nanosheet nanocomposites as the electro-catalyst was used to detect benzoic acid using cyclic voltammetry (CV) method. The nanocomposites modified GCE shows the limit of detection (LOD) of 0.56 μM and linear range of 0.001-2 mM. The polythiophene/copper bismuthate nanosheet nanocomposites can be used as good electrode materials for benzoic acid detection

Keywords: Polythiophene, Copper bismuthate nanosheets, Composites, Electrochemical detection, Benzoic acid.

1. INTRODUCTION

Benzoic acid is effective to inhibit yeast growth and against bacteria attack which is widely applied as the preservative [1-4]. However, benzoic acid is seriously harmful to human and can cause

fungal skin diseases, such as athlete's foot, tinea and ringworm at higher than permitted levels [5-7]. Therefore, the detection of benzoic acid is important for the quality assurance purposes to protect human and environment. High performance liquid chromatography technology [8,9] and on-line pyrolytic methylation technology [10] were developed to determine benzoic acid with the limit of detection (LOD) of 1.8 μM and 0.8 μM, respectively. These analytical methods still take complex measurement process and expensive apparatus. Electrochemical analytical method using different species of electrode materials has been developed for the determination of benzoic acid [11,12] taking the advantages of simple, rapid measurement process and low cost [13-17]. However, the electrochemical detection performance for benzoic acid is still expected to be enhanced by exploring novel and efficient electrode materials.

Bismuth-containing nanoscale materials show promising application in the fields of functional devices due to their good chemical and physical properties [18-22]. Bismuthate materials with different size, morphologies and compositions, as important bismuth-containing materials, have attracted great attention owing to their excellent photocatalytic, electrochemical and electronic performance for the promising application in the fields of catalysis, sensors and electronics devices [23-28]. For example, Serpone *et al.* [29] reported the synthesis of the perovskite-like barium bismuthate with rhombohedral $Ba_{1.264(4)}Bi_{1.971(4)}O_4$ phase by a solid state synthesis route. The obtained barium bismuthate possessed lower-energy indirect band gap of 2.28 eV and higher-energy direct band gap of 2.36 eV exhibiting good photocatalytic performance toward the photo-reduction of carbon dioxide. Sodium bismuthate dehydrate was prepared by a simple oil bath method and showed superior photocatalytic activity toward Rhodamine B (RhB) with visible light irradiation [30]. Zn bismuthate nanorods with cubic $ZnBi_{38}O_{58}$ phase and length of 2-10 μm, diameter of 40-250 nm were synthesized by us via a simple and green hydrothermal process [31]. The obtained Zn bismuthate nanorods exhibited good electrochemical sensing performance for L-cysteine detection with a linear range of 0.0001-2 mM and LOD of 0.074 μM. Zn bismuthate nanoscale materials with other morphologies, such as Zn bismuthate nanobundles also showed good electrochemical sensing performance for the determination of 4-nitrophenol with the LOD of 0.035 μM [32] and visible light photocatalytic activity for the degradation of azo dye pollutants [33]. Copper-containing materials exhibited good application potential in the fields of sensors, catalysis and electronic devices [34-39]. Copper bismuthate nanosheets were developed as a kind of electrode materials exhibiting good electrochemical sensing performance [40]. However, the electrochemical performance of the copper bismuthate nanosheets is expected to further be improved.

The physical and chemical properties of single phase nanoscale materials can be efficiently enhanced by the combination with other nanoscale materials [41-46]. It has been shown that different species of polymers can efficiently enhance the electrochemical performance of the electrode materials by forming compounds [47-50]. Polythiophene is a kind of typical polymers, and consists of extended π-conjugated structure and sp^2 hybridized structure resulting in the delocalization of π-electrons along polymer chain and providing good electronic performance [51]. Polythiophene can efficiently enhance the sensing performance by forming nanoscale composites with inorganic nanomaterials [52]. The combination of the nanomaterials with the polythiophene induces high sensitivity and selectivity leading to the performance enhancement of the sensors [53]. Therefore, it is expected to obtain good

electrochemical sensing performance for the detection of biological molecules by the combination of the copper bismuthate nanosheets and polythiophene. *In-situ* polymerization route is an efficient method for the fabrication of the nanocomposites [54-58]. In this research, the *in-situ* polymerization method was used to obtain polythiophene/copper bismuthate nanosheet nanocomposites. The obtained nanocomposites were analyzed by X-ray diffraction (XRD) and transmission electron microscopy. The electrochemical sensing performance of the nanocomposites for the determination of benzoic acid was studied in detail. The polythiophene/copper bismuthate nanosheet nanocomposites are expected to be used as good electrode materials for the electrochemical detection of benzoic acid.

2. EXPERIMENTAL PROCEDURE

Copper bismuthate nanosheets were obtained by the hydrothermal process using cupric iodide and sodium bismuthate as the raw materials which was described elsewhere [40]. Cupric iodide, sodium bismuthate, thiophene, methenyl trichloride, sulphuric acid, sodium hydroxide, KCl, ethanol and benzoic acid were of A.R. grade and obtained from Sinopharm Chemical Reagent Co., Ltd. of P. R. China. All solution was obtained with distilled water.

Copper bismuthate nanosheets and thiophene monomer were added into 20 mL methenyl trichloride with stirring. The mass ratio of thiophene and copper bismuthate nanosheets is 2:8. After stirring for half an hour, iron trichloride was added into the above mixed solution with continous stirring. The mole ratio of iron trichloride and thiophene was 2.4. The polymerization process lasted for 3 h at 0 ℃ and grey products were washed using alcohol and distilled water, respectively for several times and dried at 80 ℃ under vacuum.

XRD pattern of the polythiophene/copper bismuthate nanosheet nanocomposites was obtained on Bruker AXS D8 X-ray diffractometer with Cu K_α radiation (λ=1.5406 Å). The morphology and microstructure of the polythiophene/copper bismuthate nanosheet nanocomposites were analyzed by JEOL JEM-2100 high-resolution transmission electron microscopy at an accelerating voltage of 200 kV. Transmission electron microscopy sample was prepared by putting several drops of suspension solution with polythiophene/copper bismuthate nanosheet nanocomposites onto a copper grid with porous carbon film.

The polythiophene/copper bismuthate nanosheet nanocomposites were dispersed into N,N-dimethylformamide (DMF) with stirring for 1 hour to obtain homogenous nanocomposites suspension. A glassy carbon electrode (GCE) with the diameter of 3 mm was polished using 0.05 μm alumina slurries. The polished GCE was cleaned by the ultra-sonication in alcohol and distilled water, respectively. 10 μL suspension with polythiophene/copper bismuthate nanosheet nanocomposites was deposited onto the surface of the bare GCE. Then the GCE was dried using an infrared lamp. Cyclic voltammetry (CV) was used to investigate the electrochemical sensing performance of the polythiophene/copper bismuthate nanosheet nanocomposites. Benzoic acid was used as the analyte. The electrochemical sensing experiments were performed using a CHI604D electrochemical instrument (Shanghai Chenhua Company, P. R. China). Polythiophene/copper bismuthate nanosheet nanocomposites were used as the working electrode. Saturated calomel electrode (SCE) and Pt wire

were used as the reference electrode and counter electrode, respectively. The electrode system was immersed in 0.1 M KCl buffer solution containing benzoic acid with various concentrations. The applied potential was in the range from -1.0 V to +1.0 V. The cyclic voltammetric measurements were performed using various scan rates.

3. RESULTS AND DISCUSSION

The phase of the polythiophene/copper bismuthate nanosheet nanocomposites was analyzed by XRD. Figure 1 shows the XRD patterns of the copper bismuthate nanosheets and polythiophene/copper bismuthate nanosheet nanocomposites. The XRD diffraction peaks of the nanocomposites are consistent with those of the copper bismuthate nanosheets. All diffraction peaks can be ascribed to tetragonal $CuBi_2O_4$ phase (JCPDS card, PDF No. 42-0334). The result shows that the polythiophene/copper bismuthate nanosheet nanocomposites are composed of tetragonal $CuBi_2O_4$ phase.

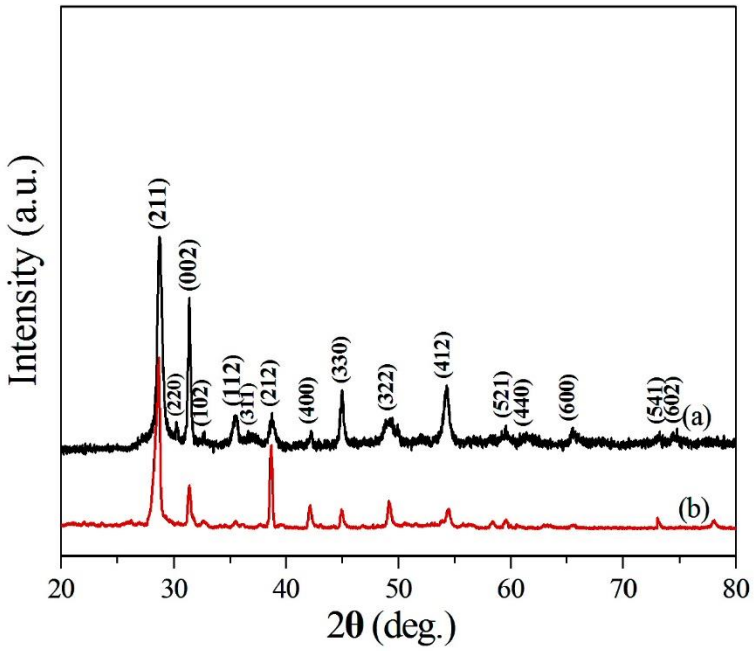

Figure 1. XRD patterns of the copper bismuthate nanosheets and polythiophene/copper bismuthate nanosheet nanocomposites. (a) Copper bismuthate nanosheets, (b) polythiophene/copper bismuthate nanosheet nanocomposites.

The size, morphology and microstructure of the polythiophene/copper bismuthate nanosheet nanocomposites were investigated by TEM and HRTEM. TEM image (Figure 2a) shows that the products are composed of sheet-shaped morphology with the size of several hundreds of nanometers which is similar to that of the copper bismuthate nanosheets [40]. It is obviously seen that some irregular polythiophene nanoscale particles are firmly attached to the surface of the copper bismuthate nanosheets which is similar to the nanocomposites reported by us in previous research [59,60].

HRTEM image (Figure 2b) shows that the nanocomposites have clear lattice fringes with different directions which belong to polycrystalline tetragonal $CuBi_2O_4$ structure. Amorphous polythiophene nanoparticles attach to the surface of the polycrystalline copper bismuthate nanosheets. The results confirm the formation of the nanocomposites with polythiophene and copper bismuthate nanosheets.

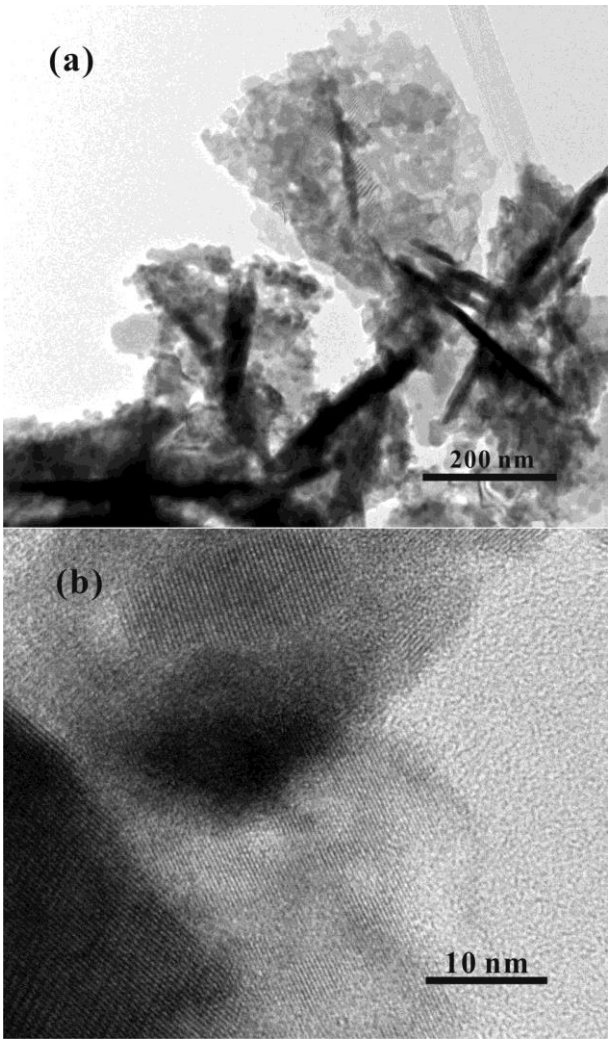

Figure 2. Transmission electron microscopy of the polythiophene/copper bismuthate nanosheet nanocomposites. (a) TEM, (b) HRTEM.

The formation of the polythiophene/copper bismuthate nanosheets nanocomposites is proposed according to an *in-situ* oxidative polymerization process. Based on the *in-situ* polymerization route, iron trichloride and thiophene serve as the oxidizing agent and monomer, respectively. Iron trichloride was directed added to the thiophene solution and methenyl trichloride solution with the copper bismuthate nanosheets and thiophene was sonicated. Thiophene monomers were adsorbed to the surface of the copper bismuthate nanosheets. Iron trichloride induces the thiophene monomer to form the covalent bonds between the thiophene units [61]. Thiophene monomers polymerize at the surface of the copper bismuthate nanosheets resulting in the formation of the polythiophene/copper bismuthate nanosheet nanocomposites.

The polythiophene/copper bismuthate nanosheet nanocomposites were used as the GCE modified materials for the electrochemical determination of benzoic acid. The CVs of 2 mM benzoic acid at different electrodes were firstly investigated which is shown in Figure 3.

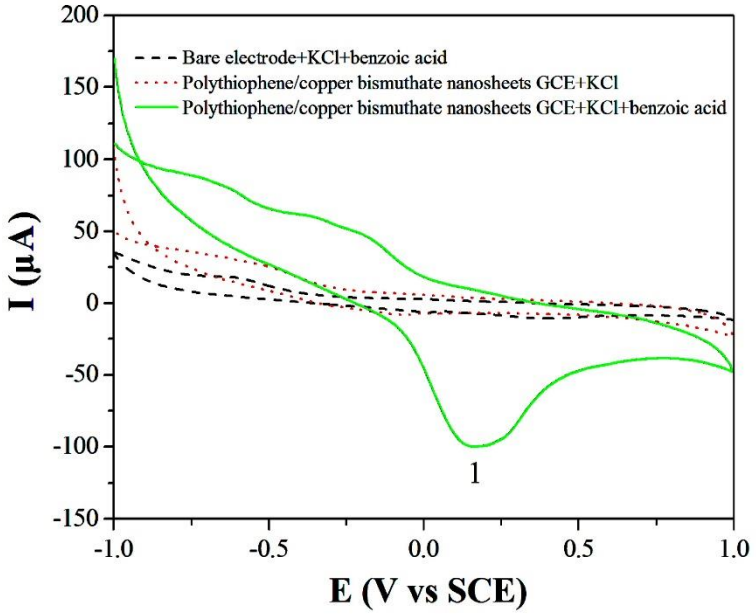

Figure 3. CV of 2 mM benzoic acid in 0.1 M KCl buffer solution at bare electrode. CVs in 0.1 M KCl buffer solution at the polythiophene/copper bismuthate nanosheet nanocomposites modified GCE with and without 2 mM benzoic acid. Scan rate, 50 $mV \bullet s^{-1}$.

It is shown that no electrochemical CV peaks are observed from the CV of 2 mM benzoic acid in 0.1 M KCl buffer solution at bare electrode. This shows that bare electrode has no electro-catalytic activity towards benzoic acid which is consistent with previous reports [16,17]. There are no CV peaks observed from the CV at the polythiophene/copper bismuthate nanosheet nanocomposites modified GCE in 0.1 M KCl buffer solution without benzoic acid. Different from the above CVs, an irreversible CV peak located at + 0.17 V is observed from the CV at the polythiophene/copper bismuthate nanosheet nanocomposites modified GCE in 0.1 M KCl buffer solution with 2 mM benzoic acid. The electrochemical CV peaks can only be observed from the nanocomposites modified GCE in the mixed solution with KCl and benzoic acid showing that the CV peak originates from the polythiophene/copper bismuthate nanosheet nanocomposites. The irreversible CV peak is very different from the CV peaks located at +0.13 V, +0.05 V and -0.06 V, -0.82 V at the copper vanadate nanobelts modified GCE in 0.1 M KCl buffer solution with 2 mM benzoic acid [17]. It was also reported that only an irreversible electrochemical CV peak was formed at +0.29 V at the polynaphthylamine/graphene composites modified GCE [62]. However, the potential of the CV peak is lower than that at the polynaphthylamine/graphene composites modified GCE. The result shows that the polythiophene/copper bismuthate nanosheet nanocomposites possess superior electro-catalytic performance for benzoic acid. It has been reported that the electrochemical CV peaks were ascribed to the oxidation-reduction process of benzoic acid [16,17]. Only an irreversible CV peak is observed at the nanocomposites modified electrode which can be attributed to the oxidation process of benzoic

acid.

It has been reported that pH value of the buffer solution plays important role in the electrochemical behaviors of biological molecules at the nanomaterials modified GCE [63-65]. Therefore, pH value of the buffer solution was adjusted to investigate the electrochemical behaviors of the nanocomposites modified GCE in the mixed solution of 0.1 M KCl and 2 mM benzoic acid.

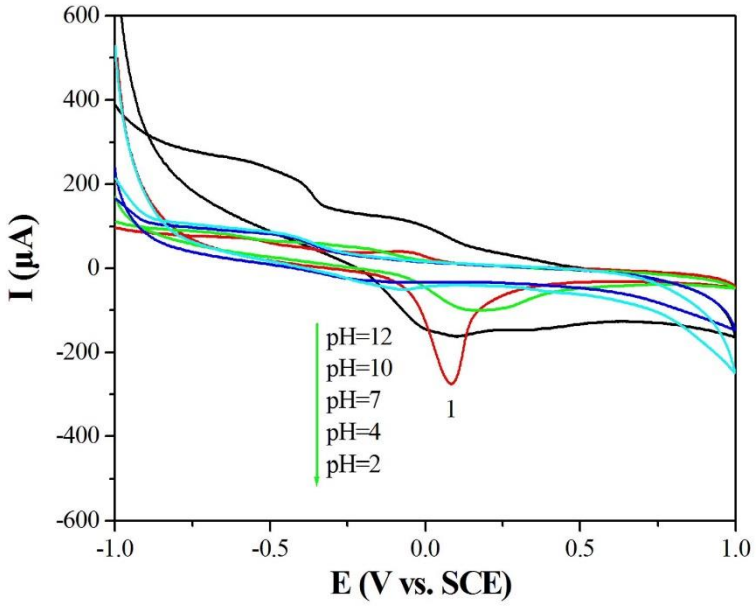

Figure 4. Influence of the pH value on the CVs of 2 mM benzoic acid in 0.1 M KCl buffer solution at the polythiophene/copper bismuthate nanosheet nanocomposites modified GCE. Scan rate, 50 $mV•s^{-1}$.

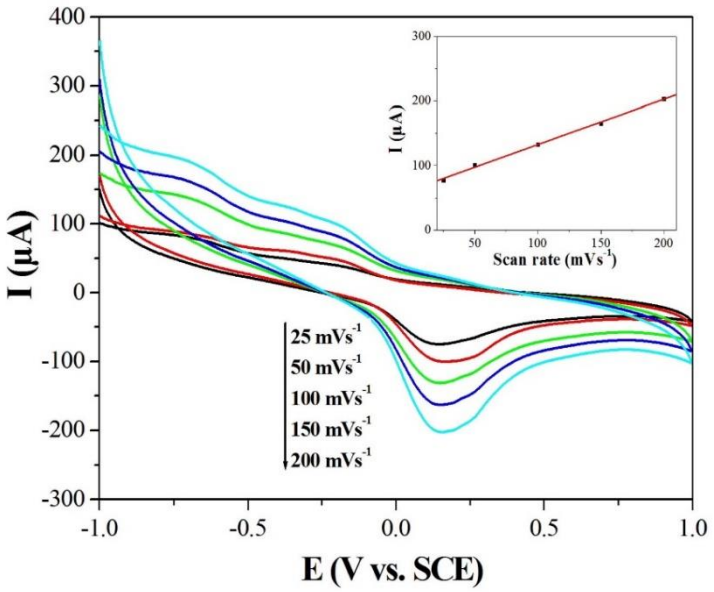

Figure 5. Influence of the scan rate on the CVs of 2 mM benzoic acid in 0.1 M KCl buffer solution at the polythiophene/copper bismuthate nanosheet nanocomposites modified GCE. Scan rate, 50 $mV•s^{-1}$. The plot between the intensity of the CV peak and scan rate is shown in the inset of the upper-right part.

Figure 4 shows the CVs of 2 mM benzoic acid in 0.1 M KCl buffer solution at the polythiophene/copper bismuthate nanosheet nanocomposites modified GCE. It is obviously observed that the intensity of the electrochemical CV peak increases and the potential of the CV peak shifts to negative direction with increasing the acidity of the buffer solution. The results show that the nanocomposites modified GCE has superior electro-catalytic activity toward benzoic in acidic buffer solution and hydrogen ions take part in the oxidation process of benzoic acid.

The electrochemical kinetics of the polythiophene/copper bismuthate nanosheet nanocomposites modified GCE for benzoic acid detection has been investigated by adjusting the scan rate from 25 $mV•s^{-1}$ to 200 $mV•s^{-1}$.

Figure 5 shows the CVs of 2 mM benzoic acid in 0.1 M KCl buffer solution at the nanocomposites modified GCE using various scan rates. The current of the CV peak increases obviously by improving the scan rate. There is a linear relationship between the intensity of the CV peak and scan rate (see the inset of the upper-right part of Figure 5) with the correlation coefficient R of 0.998. The result shows that the oxidation process of benzoic acid at the polythiophene/copper bismuthate nanosheet nanocomposites modified GCE is controlled by a surface adsorption process [66,67].

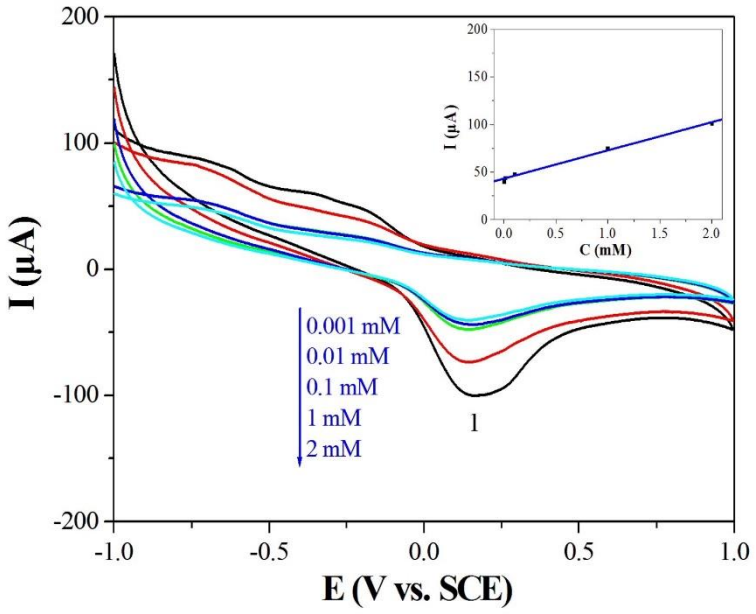

Figure 6. Influence of the benzoic acid concentration on the CVs of benzoic acid in 0.1 M KCl buffer solution at the polythiophene/copper bismuthate nanosheet nanocomposites modified GCE. Scan rate, 50 $mV•s^{-1}$. The plot between the intensity of the CV peak and benzoic acid concentration is shown in the inset of the upper-right part.

The LOD, linear range and correlation coefficient were determined by investigating the CVs of benzoic acid with different concentrations in 0.1 M KCl buffer solution at the polythiophene/copper bismuthate nanosheet nanocomposites modified GCE (Figure 6). There is a linear relationship between the intensity of the CV peak and benzoic acid concentration (see the inset in the upper-right part of Figure 6). The regression equation is calculated to be I_p=43.524+29.533C, where I_p refers to the current

of the CV peak (μA), *C* refers to benzoic acid concentration (mM). The LOD is calculated to be 0.56 μM based on S/N=3. The linear range and correlation coefficient are 0.001-2 mM and 0.997, respectively. Comparing with other methods and electrodes for the determination of benzoic acid (Table 1), the polythiophene/copper bismuthate nanosheet nanocomposites modified GCE shows wide linear range and comparable LOD. The polythiophene/copper bismuthate nanosheet nanocomposites exhibit good electro-catalytic activity towards benzoic acid.

Table 1. Performance comparison using different methods and electrodes for the determination of benzoic acid.

Methods and electrodes	Linear range (mM)	LOD (μM)	References
Electrochemical method by polyphenol oxidase electrode	Up to 20	0.2	5
Copper germanate/polyaniline nanowire modified GCE	0.001-2	0.43	6
High performance liquid chromatography	0.041-0.983	4.1	7
High performance liquid chromatography	0.004-0.123	1.8	8
GCE with on-line pyrolytic methylation technique	0.008-80	0.8	10
Electrochemical method by mushroom tissue homogenate electrode	0.001-0.04	0.9	16
Copper vanadate nanobelts modified GCE	0.001-2	0.61	17
Polynaphthylamine/graphene composites modified GCE	0.001-2	0.34	62
Polythiophene/copper bismuthate nanosheet nanocomposites modified GCE	0.001-2	0.56	This work

The repeatability of the polythiophene/copper bismuthate nanosheet nanocomposites modified GCE for the determination of benzoic acid has been investigated by the cyclic measurement of the CV of 2 mM benzoic at the nanocomposites modified GCE. The CVs of 2 mM benzoic acid in 0.1 M KCl buffer solution at the nanocomposites modified GCE for the 1st and 20th time are shown in Figure 7. The relative standard deviation (R.S.D.) is 3.79% exhibiting good repeatability of the nanocomposites modified GCE.

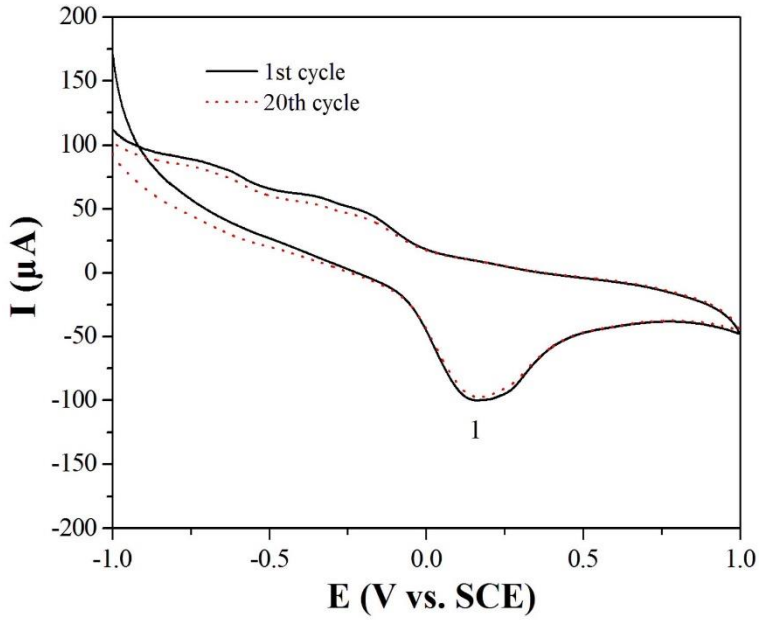

Figure 7. CVs of 2 mM benzoic acid in 0.1 M KCl buffer solution at the polythiophene/copper bismuthate nanosheet nanocomposites modified GCE for the 1st and 20th time, respectively. Scan rate, 50 $mV \bullet s^{-1}$.

As the practical application, polythiophene/copper bismuthate nanosheet nanocomposites modified GCE has been used to detect benzoic acid in tap water samples (Table 2). The benzoic acid concentration in the tap water samples is 5.0, 20.0 and 40.0 μM, respectively. The real sample measurements were performed at room temperature. The measured values were calculated from five separate measurements and recovery of benzoic acid was determined by standard addition. The results suggest that the polythiophene/copper bismuthate nanosheet nanocomposites modified GCE is reliable and sensitive with regard to determining benzoic acid.

Table 2. Electrochemical determination of benzoic acid using polythiophene/copper bismuthate nanosheet nanocomposites modified GCE in tap water.

Sample (Tap water)	Amount added (μM)	Amount found (μM) (average of five times)	Recovery (%)
1	5.0	5.0±0.2	98.2
2	20.0	19.9±0.3	99.3
3	40.0	40.9±0.3	103.6

4. CONCLUSIONS

In summary, polythiophene/copper bismuthate nanosheet nanocomposites were obtained by an *in-situ* polymerization route. The obtained nanocomposites possess polycrystalline tetragonal $CuBi_2O_4$

phase and amorphous polythiophene nanoparticles attach to the surface of the copper bismuthate nanosheets. The polythiophene/copper bismuthate nanosheet nanocomposites modified GCE possesses superior electro-catalytic activity towards benzoic acid with increasing the acidity and scan rate. The nanocomposites modified GCE shows low LOD of 0.56 μM and wide linear range of 0.001-2 mM. The nanocomposites modified electrode shows good electrochemical sensing performance for the detection of benzoic acid.

ACKNOWLEDGMENTS
This work was supported by the Major Scientific Instrument Development Project of National Natural Science Foundation of China (No. 41627801), Natural Science Foundation of Anhui Province of P. R. China (2008085ME172), Natural Science Foundation of Fujian Province of P. R. China (2019J01872) and Student Innovation and Entrepreneurship Training Program of P. R. China (202010360021).

References

1. M. U. Faroque, A. Mehmood, S. Noureen and M. Ahmed, *J. Mol. Struct.*, 1214 (2020) 128183.
2. J. L. Zhang, J. R. Zhai, H. Zheng, X. Y. Li, Y. R. Wang, X. P. Li and B. S. Xing, *Sci. Total Environ.*, 738 (2020) 139685.
3. L. Z. Pei, F. L. Qiu, Y. Ma, F. F. Lin, C. G. Fan and X. Z. Ling, *Curr. Pharm. Anal.*, 16 (2020) 153.
4. L. C. Chen, W. Cui, J. Y. Li, H. Wang, X. A. Dong, P. Chen, Y. Zhou and F. Dong, *Appl. Catal. B: Environ.*, 271 (2020) 118948.
5. D. Shan, Q. F. Shi, D. B. Zhu and H. G. Xue, *Talanta*, 72 (2007) 1167.
6. L. Z. Pei, Z. Y. Cai, Y. K. Xie and D. G. Fu, *Measurement*, 53 (2014) 62.
7. B. Saad, M. F. Bari, M. I. Saleh, K. Ahmad and M. K. M. Talib, *J. Chromatogr. A.*, 1073 (2005) 393.
8. C. Y. Liu, B. Qin, J. Zhang, Y. M. Wei, Y. Q. Miao and H. Zhang, *Proceedings of 2009 Internationgal Conference of Natural Product and Traditional Medicine*, (2009) 296.
9. N. Tungkijanansin, W. Alahmad, T. Nhujak and P. Varanusupakul, *Food Chem.*, 329 (2020) 127161.
10. Z. Pan, L. Wang, W. Mo, C. Wang, W. Hu and J. Zhang, *Anal. Chim. Acta.*, 545 (2005) 218.
11. J. X. Pei, X. Yu, Z. Q. Zhang, J. Zhang, S. B. Wei and R. Boukherroub, *Appl. Surf. Sci.*, 527 (2020) 146761.
12. H. Zhang, Y. S. Wang, D. W. Zhao, D. D. Zeng and J. Y. Xia, *ACS Appl. Mater. Interf.*, 7 (2015) 16152.
13. L. Z. Pei, T. Wei, N. Lin and H. Zhang, *J. Alloy. Compd.*, 663 (2016) 677.
14. Y. K. Xie, L. Z. Pei, Y. Q. Pei and Z. Y. Cai, *Measurement*, 47 (2014) 341.
15. L. Z. Pei, Y. Q. Pei, Y. K. Xie, C. G. Fan and Q. F. Zhang, *Int. J. Mater. Res.*, 104 (2013) 1267.
16. M. D. Morales, S. Morante, A. Escarpa, M. C. Gonzalez, A. J. Reviejo and J. M. Pingarron, *Talanta*, 57 (2002) 1189.
17. N. Lin, L. Z. Pei, T. Wei, H. D. Liu and Z. Y. Cai, *IET Sci. Meas. Technol.*, 10 (2016) 247.
18. H. B. Li, J. Zhang, G. Y. Huang, S. H. Fu, C. Ma, B. Y. Wang, Q. R. Huang and H. W. Liao, *Trans. Nonferrous Met. Soc. China*, 27 (2017) 868.
19. T. X. Fu, *Mater. Res. Bull.*, 99 (2018) 460.
20. L. Z. Pei, J. F. Wang, Y. P. Dong, X. X. Tao, S. B. Wang, C. G. Fan, J. L. Hu and Q. F. Zhang, *Curr. Nanosci.*, 7 (2011) 402.
21. L. Z. Pei, T. Wei, N. Lin and H. Y. Yu, *Int. J. Mater. Res.*, 107 (2016) 477.

22. S. Y. Cao, C. S. Chen, X. D. Xi, B. Zeng, X. T. Ning, T. G. Liu, X. H. Chen, X. M. Meng and Y. Xiao, *Vacuum*, 102 (2014) 1.
23. D. S. Shtarev, A. V. Shtareva and M. S. Molokeev, *Key Eng. Mater.*, 806 (2019) 161.
24. L. Z. Pei, T. Wei, N. Lin, C. G. Fan and Z. Yang, *J. Alloy. Compd.*, 679 (2016) 39.
25. K. Rokesh, M. Sakar and T. O. Do, *ChemPhotoChem*, (2020) DOI: 10.1002/cpt.201900265.
26. L. Z. Pei, F. F. Lin, F. L. Qiu, W. L. Wang, Y. Zhang and C. G. Fan, *Mater. Res. Express*, 4 (2017) 075047.
27. M. Saiduzzaman, S. Akutsu, N. Kumada, T. Takei, S. Yanagida, H. Yamane and Y. Kusano, *Inorg. Chem.*, (2020) DOI: https://dx.doi.org/10.1021/acs.inorgchem.0c00213.
28. F. L. Qiu, Z. Wang, H. J. Chen, Y. Ma, H. Wu, L. Yan, L. Z. Pei and C. G. Fan, *Curr. Nanosci.*, (2020) DOI: 10.2174/1573413715666191212153902.
29. D. S. Chtarev, A. V. Shtareva, R. Kevorkyants, A. V. Rudakova, M. S. Molokeev, T. V. Bakiev, K. M. Bulanin, V. K. Ryabchuk and N. Serpone, *J. Mater. Chem. C*, 8 (2020) 3509.
30. Y. T. Feng, X. M. Huang, Q. F. Zhan and D. M. Jiang, *J. Mater. Sci: Mater. Electron.*, 30 (2019) 10543.
31. L. Z. Pei, T. Wei, N. Lin, Z. Y. Cai, C. G. Fan and Z. Yang, *J. Electrochem. Soc.*, 163 (2016) H1.
32. A. Padmanaban, T. Dhanasekaran, R. Manigandan, S. P. Kumar, G. Gnanamoorthy, A. Stephen and V. Narayanan, *New J. Chem.*, 41 (2017) 7020.
33. H. Najafian, F. Manteghi, F. Beshkar and M. Salavati-Niasari, *Sep. Purif. Technol.*, 195 (2018) 30.
34. L. Z. Pei, L. J. Yang, Y. Yang, C. Z. Yuan, C. G. Fan and Q. F. Zhang, *Mater. Chem. Phys.*, 130 (2011) 104.
35. H. B. Li, P. Jiang, W. B. Zhang, S. G. Chen and F. J. Li, *Nanosci. Nanotechnol. Lett.*, 10 (2018) 451.
36. L. Z. Pei, J. F. Wang, L. J. Yang, S. B. Wang, Y. P. Dong, C. G. Fan and Q. F. Zhang, *Mater. Charact.*, 62 (2011) 354.
37. N. Lin, L. Z. Pei, T. Wei and H. Y. Yu, *Cryst. Res. Technol.*, 50 (2015) 255.
38. L. Jia, H. Yang, J. M. Chen, Y. Zhou, P. Ding, L. G. Li, N. Han and Y. G. Li, *Chin. J. Chem.*, 37 (2019) 497.
39. N. Kumada, A. Nakamura, A. Miura, T. Takei, M. Azuma, H. Yamamoto, E. Magome, C. Moriyoshi and Y. Kuroiwa, *J. Solid State Chem.*, 245 (2017) 30.
40. Y. Zhang, F. F. Lin, T. Wei and L. Z. Pei, *J. Alloy. Compd.*, 723 (2017) 1062.
41. W. W. Yu, X. A. Chen, W. Mei, C. S. Chen and Y. H. Tsang, *Appl. Surf. Sci.*, 400 (2017) 129.
42. J. F. Duan, C. Zhu, Y. H. Du, Y. L. Wu, Z. Y. Chen, L. J. Li, H. L. Zhu and Z. Y. Zhu, *J. Mater. Sci.*, 52 (2017) 10470.
43. C. S. Chen, W. W. Yu, T. G. Liu, S. Y. Cao and Y. H. Tsang, *Sol. Energ. Mat. Sol. C.*, 160 (2017) 43.
44. W. Z. Huang, X. Y. Gan and L. Zhu, *Ceram. Int.*, 44 (2018) 5473.
45. C. S. Chen, S. Y. Cao, W. W. Yu, X. D. Xie, Q. C. Liu, Y. H. Tsang and Y. Xiao, *Vacuum*, 116 (2015) 48.
46. L. Z. Pei, F. L. Qiu, Y. Ma, F. F. Lin, C. G. Fan, X. Z. Ling and S. B. Zhu, *Fuller. Nanotub. Car. N.*, 27 (2019) 58.
47. J. Wang, D. Fu, B. Q. Ren, P. Yu, X. C. Zhang, W. J. Zhang and K. Kan, *RSC Adv.*, 9 (2019) 23109.
48. L. Z. Pei, H. D. Liu, N. Lin, Y. K. Xie and Z. Y. Cai, *Curr. Pharm. Anal.*, 11 (2015) 16.
49. S. M. Zhao, H. X. Chen, J. L. Li and J. X. Zhang, *New J. Chem.*, 43 (2019) 15014.
50. L. Z. Pei, Y. Yang, Y. Q. Pei and Y. K. Xie, *Recent Pat. Nanotechnol.*, 7 (2013) 93.
51. Z. Q. Liang, M. M. Li, Q. Wang, Y. P. Qin, S. J. Stuard, Z. X. Peng, Y. F. Deng, H. Ade, L. Ye and Y. H. Geng, *Joule*, (2020) DOI: https://doi.org/10.1016/j.joule.2020.04.014.
52. S. L. Bai, K. W. Zhang, J. H. Sun, D. F. Zhang, R. X. Luo, D. Q. Li and C. C. Liu, *Sens. Actuat. B: Chem.*, 197 (2014) 142.
53. N. N. Linh, T. T. T. Duong, N. Hien and V. Q. Trung, *Vietnam J. Chem.*, 58 (2020) 1.

54. J. Wan, Y. Si, C. Li and K. Zhang, *Anal. Methods*, 8 (2016) 3333.
55. L. Z. Pei, Y. Ma, F. L. Qiu, F. F. Lin, C. G. Fan and X. Z. Ling, *Curr. Anal. Chem.*, 16 (2020) 493.
56. H. J. Chen, F. F. Lin, C. H. Yu, Z. Y. Xue, Z. Wang, L. Z. Pei, H. Wu, P. X. Wang, Q. M. Cong, C. G. Fan and X. Z. Ling, *Int. J. Electrochem. Sci.*, 15 (2020) 1742.
57. L. Z. Pei, S. Wang, H. D. Liu and Y. Q. Pei, *Recent Pat. Nanotechnol.*, 8 (2014) 142.
58. H. Zhu, L. Ma, J. Jiang, Z. M. Xia, X. He, J. Yang, B. D. Yang and Q. Li, *Int. J. Electrochem. Sci.*, 15 (2020) 371.
59. L. Z. Pei, Z. Y. Cai, Y. K. Xie, Y. Q. Pei, C. G. Fan and D. G. Fu, *J. Electrochem. Soc.*, 159 (2012) G107.
60. L. Z. Pei, F. L. Qiu, Y. Ma, F. F. Lin, C. G. Fan and X. Z. Ling, *Curr. Nanosci.*, 15 (2019) 492.
61. M. A. Memon, J. H. Sun, H. T. Jung, S. K. Yan and J. X. Geng, *Chin. J. Polym. Sci.*, 35 (2017) 422.
62. L. Z. Pei, Y. Ma, F. L. Qiu, F. F. Lin, C. G. Fan and X. Z. Ling, *Mater. Res. Express*, 6 (2019) 015053.
63. B. Zhang, Q. Wu, B. Li, X. Tang, F. Ju, Q. Q. Yang, Q. H. Wang and Y. L. Zhou, *Int. J. Electrochem. Sci.*, 15 (2020) 137.
64. L. Z. Pei, Y. Q. Pei, Y. K. Xie, C. G. Fan and H. Y. Yu, *CrystEngComm*, 15 (2013) 1729.
65. L. Z. Pei, T. Wei, N. Lin, H. Zhang and C. G. Fan, *Russ. J. Electrochem.*, 54 (2018) 84.
66. L. Z. Pei, N. Lin, T. Wei, H. D. Liu and H. Y. Yu, *J. Mater. Chem. A*, 3 (2015) 2690.
67. Z. Xia, Y. Zhang, Q. Z. Li, H. J. Du, G. F. Gui and G. Y. Zhao, *Int. J. Electrochem. Sci.*, 15 (2020) 559.